Appl Petrochem Res (2013) 3:35–45
DOI 10.1007/s13203-013-0027-9

ORIGINAL ARTICLE

Propan-2-ol conversion to diisopropyl ether over $(NH_4)_xX_yPMo_{12}O_{40}$ salts with X = Sn, Sb, and Bi. The effect of salt preparation pH

F. Chami · L. Dermeche · A. Saadi · C. Rabia

Received: 19 December 2012 / Accepted: 14 May 2013 / Published online: 18 June 2013

Abstract $(NH_4)_3PMo_{12}O_{40}$ and $(NH_4)_xX_yPMo_{12}O_{40}$ mixed salts (X: Sn, Sb and Bi) were prepared at pH 4 and characterised by IR, Raman and UV–Vis spectroscopies, ^{31}P NMR, XRD, BET and thermal analysis (TG and DTA). The different salts were tested in propan-2-ol decomposition at 100 °C, after pretreatment in situ under nitrogen stream in 150–250 °C temperature range. Their properties were compared with those of $(NH_4)_3PMo_{12}O_{40}$, prepared at pH 1. The salts are active and the distribution of reaction products (propene, diisopropyl ether (DIPE) and acetone) depends both on the operating conditions and the catalyst composition. Propene selectivity increases from ca. 23 to ca. 95 % with the pretreatment temperature for all catalysts. The comparison of catalytic behaviour of salts for a pretreatment temperature of 200 °C shows that they are selective towards DIPE and that among them, $SbPMo_{12}$ is the most selective one (ca. 72 %). The acetone, a dehydrogenation product, is mainly observed for salts prepared at pH 4, when the pretreatment temperature is low (150 °C) with selectivities of ca. 32–65 %.

Keywords Keggin anions · Propan-2-ol · Diisopropyl ether · Dehydration · Oxygenated additives

F. Chami · L. Dermeche · A. Saadi · C. Rabia (✉)
Laboratoire de Chimie du Gaz Naturel, Faculté de Chimie, Université des Sciences et de la Technologie Houari Boumediène, USTHB, BP32, El-Alia, 16111 Bab-Ezzouar, Algiers, Algeria
e-mail: c_rabia@yahoo.fr; crabia@usthb.dz

Introduction

Alcohols and ethers are used as oxygenated additives to motor fuels and as antiknock components in gasoline. They increase the octane number and reduce the emissions of gases to greenhouse effect (CO_x and NO_x). These oxygenated compounds have partially replaced the lead-based salts that are toxic and pollutant. Among the tertiary ethers, such as ethyl tertiary butyl ether, tertiary amyl ethyl ether and tertiary amyl methyl ether, MTBE is the oxygenated additive currently, the most widely used in the reformulated gasoline and also one of organic chemicals the most produced industrially [1]. However, the major drawback of this ether is its easy diffusion in the ground water, its slow biological breakdown and its unpleasant odour. The diisopropyl ether (DIPE) can be a potential candidate to substitute the MTBE. It has the advantage to increase the octane number and to have a lower vapour pressure. Various works proposed the synthesis of the DIPE from propene and water in a two-stage process [2], from a feed of acetone and hydrogen in a two-stage process [3] or one-step process [4] and from acetone feedstock [5]. The DIPE can be also synthesised either from a feed of propylene and water [6] or from a feed of propene and isopropanol over an acidic ion exchange resin like Amberlyst 15 [7]. The synthesis of the DIPE from the isopropanol decomposition was examined over aluminosilicates supported sulfopolyphenylketone (or polyphenylketone) [8] and over sulphated titania [9].

The use of polyoxometalates and particularly those having the Keggin structure as solid catalysts offer strong option for efficient and cleaner process compared with polluting corrosive liquid catalysts as conventional mineral acids and highly acidic resins like Amberlyst. It is well known that Keggin-type heteropoly acids (HPAs) are

strong Brönsted acids and that they catalyse a wide variety of reactions in homogeneous and heterogeneous phases. Among the heteropoly acids, $H_3PW_{12}O_{40}$ and $H_4SiW_{12}O_{40}$ were found effective in MTBE [10, 11] and DIPE synthesis [12]. One of the characteristics of polyoxometalates is their ability to easily absorb polar molecules, such as alcohols and ethers. The reactant molecules in the gas or liquid phase penetrate in between the polyanions and react inside the bulk solid. This concept is known as 'pseudoliquid' catalysis [13].

In this study, we have used the ammonium salt of 12-molybdophosphoric acid that is mesoporous with a large surface area and which exhibits better thermal stability than the parent acid, and we have replaced partially ammonium ions by antimony, bismuth or tin to increase the density of acid sites necessary to isopropanol dehydration. We report here the synthesis at pH 1 and 4 for $(NH_4)_3PMo_{12}O_{40}$ and at pH 4 for ammonium–antimony, $(NH_4)_xSb_yPMo_{12}O_{40}$, ammonium–bismuth, $(NH_4)_xBi_yPMo_{12}O_{40}$ and ammonium–tin, $(NH_4)_xSn_yPMo_{12}O_{40}$, mixed phosphomolybdates (noted $(NH_4)_3PMo_{12}$, $SbPMo_{12}$, $BiPMo_{12}$ and $SnPMo_{12}$, respectively) and characterization by IR, Raman and UV–Vis spectroscopies, ^{31}P NMR, BET, XRD and thermal analysis (TG and DTA). In a previous study, we prepared this series of materials at pH 1 and we characterised them using the same techniques [14]. The Keggin anion ($PMo_{12}O_{40}^{3-}$) is usually prepared at pH <1, in presence of ammonium ions, the corresponding salt, $(NH_4)_3PMo_{12}O_{40}$, precipitates. However, the preparation of $(NH_4)_3PMo_{12}O_{40}$ can be carried out at pH between 1 and 7. In this range, lacunary compounds could be developed with the composition $(NH_4)_7PMo_{11}O_{39}$ [15]. This latter could lead to a higher number of ammonium ions that can increase the acidity of solid, favourable to the isopropanol dehydration reaction.

Experimental

Catalyst synthesis

$(NH_4)_3PMo_{12}O_{40}$ and the mixed ammonium salts, $(NH_4)_xX_yPMo_{12}O_{40}$ where $X^{n+} = Sb^{3+}$, Bi^{3+} and Sn^{2+} (noted $XPMo_{12}$) were precipitated at pH 4. For each salt, a solution (A) was prepared as follows: 25 g of ammonium heptamolybdate (0.02 mol) was dissolved in 100 ml of water by heating and 1.15 ml of phosphoric acid (85 %, 0.01 mol) was added. The solution becomes pale yellow. The pH is then equal to 5.5. $(NH_4)_3PMo_{12}O_{40}$ was precipitated by slow addition of concentrated hydrochloric acid (37 %) to the solution (A) until pH 4. The yellow compound was filtered off and dried overnight at 50 °C. For the preparation of the mixed ammonium salts ($XPMo_{12}$), the solution (A) was added to 0.01 mol of XCl_3 (Sb or Bi) or XCl_2 (Sn) previously dissolved in the minimum amount of concentrated hydrochloric acid. $XPMo_{12}$ salt was precipitated by slow addition of concentrated hydrochloric acid until pH 4. The precipitate was filtered off and dried overnight at 50 °C.

Characterisation

BET surface area measurements were performed at liquid nitrogen temperature using a Micromeritics Accusorb 2100E. Prior to each adsorption–desorption measurement, the sample was degassed at $T = 130$ °C for 16 h.

Infrared spectra were recorded on a Bruker IFS 66 FT-IR spectrometer with samples prepared as KBr disks on the 400–4,000 cm^{-1} range.

Laser Raman spectroscopy data were obtained with a Kaiser Optical Systems Hololab 5000R model, equipped with near-IR laser diode ($\lambda_{exc} = 785$ nm) and CCD detector. The laser power was adjusted to 10 mW at the sample position to prevent local heating effects.

^{31}P MAS NMR spectra were measured at room temperature on a Bruker Avance 400 spectrometer. 85 % H_3PO_4 was used as an external reference.

UV–Visible diffuse reflectance spectra were recorded in the 200–800 nm regions on a Varian Cary 5E spectrometer equipped with a polytetrafluoroethylene (PTFE) integration sphere. PTFE was used as a reference.

X-ray diffraction powder patterns were obtained on a D8 Advance Bruker AXS diffractometer using Cu Kα radiation and VANTEK fast detector in HTK16 ANTON PAAR room.

Thermogravimetric and differential thermal data were collected on a SDT-2960 thermal analyzer. The thermogravimetry and differential thermal analysis experiments were performed under air flux, using 25–70 mg samples and a heating rate of 10 °C/min.

Catalytic test

Isopropanol decomposition reaction was carried out at 100 °C in a continuous flow fixed-bed Pyrex tubular reactor working at atmospheric pressure. Before each reaction, the catalyst (200 mg) was pretreated in situ for 2 h at 150–250 °C range temperatures (heating rate of 5 °C/min) under nitrogen stream with a flow of 2 l/h. A thermocouple was installed within the reactor, in contact with the catalyst bed, control the temperature. The space time in the reactor was of 0.72 s. Isopropanol partial pressure in the gas feed was adjusted to 4 kPa by the mean of a saturator followed by a condenser cooled to 273 K. Isopropanol was then introduced and passed through the catalyst by bubbling nitrogen (flow rate of 16.67 ml/min).

Reactant (isopropanol) and products (propene, diisopropyl ether and acetone) were analysed with an online gas chromatograph with a 2-m (i.d., 3 mm) column of 8 % Carbowax1540/Chromosorb (W80-100 mesh) and a flame ionization (FID) detector (Delsi ICG 121 Ml). Conversion and selectivities were measured after 5 h of reaction at each pretreatment temperature, when nearly steady-state is reached.

Results

Characterization

The BET surface areas of $(NH_4)_3PMo_{12}$, prepared at pH 1, is of 222 $m^2\ g^{-1}$. It is known that the Keggin-type salts formed with large monovalent ions, such as Cs^+, NH_4^+ or Ag^+, are insoluble in water and generally, have high surface area [13]. By contrast, $(NH_4)_3PMo_{12}$, prepared at pH 4, has a low BET surface area (17 $m^2\ g^{-1}$), evidencing thus the influence of pH parameter on the textural property of salt. However, the partial substitution of the protons by X^{n+} ions has the effect of increasing the BET surface, with 31, 74 and 158 $m^2\ g^{-1}$ for $SbPMo_{12}$, $BiPMo_{12}$ and $SnPMo_{12}$, respectively.

The FTIR spectrum of $(NH_4)_3PMo_{12}O_{40}$, prepared at pH 1 (Fig. 1a), shows the characteristic bands of the Keggin structure in the low wave number region (1,100–500 cm^{-1}). According to Rocchiccioli-Deltcheff et al. [16], the vibration bands at 1,063, 961, 863, 786 and 561 cm^{-1} correspond to $\nu_{as}(P–O_a)$, ν_{as} (Mo–O_d), ν_{as} (Mo–O_b–Mo), ν_{as} (Mo–O_c–Mo) and δ (P–O), respectively. In Keggin unit, O_a refers to O atom common to PO_4 tetrahedron and a trimetallic group: O_b to O atom connecting two trimetallic groups, O_c to O atom connecting two MoO_6 octahedrals inside a trimetallic group and O_d to the terminal O atom. In addition, the vibration band attributed to ammonium ions is observed at 1,403–1,407 cm^{-1}. The IR spectrum is not affected by the increase of pH (pH 4) as a consequence of the no modification of the Keggin anion symmetry (Fig. 1b). IR spectra of substituted salts (Fig. 2), prepared at pH 4, are similar and show that the Keggin structure was not modified.

The Raman spectra of different salts are shown in Fig. 3. The Raman spectra of $(NH_4)_3PMo_{12}$ prepared at pH 1 and pH 4 and that of $BiPMo_{12}$, in the low wave number region (1,000–240 cm^{-1}) exhibit the characteristic bands of the Keggin unit. According to literature data [17], the bands at 988, 876, 608 and 240 cm^{-1} correspond to $\nu_s(Mo=O_d)$, $\nu_{as}(M–O_b–Mo)$, $\nu_s(Mo–O_c–M)$ and $\nu_s(Mo–O_a)$ metal–oxygen vibrations, respectively. The shoulder at 971 cm^{-1} is attributed to $\upsilon_{as}(Mo=O_d)$. Its intensity is lower in the case of salts prepared at pH 4, suggesting that a pH increase has

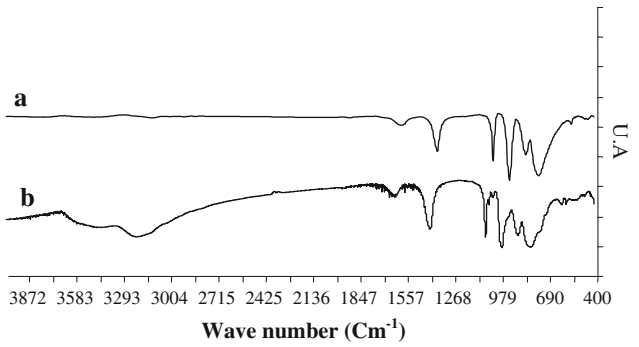

Fig. 1 FT–IR spectra of $(NH_4)_3PMo_{12}O_{40}$ *a* prepared at pH 1, *b* prepared at pH 4

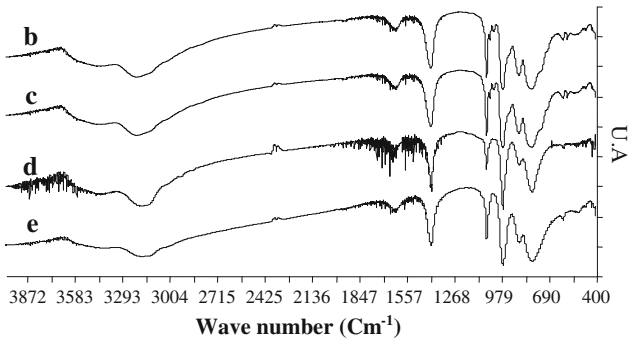

Fig. 2 FT–IR spectra of $XPMo_{12}$ *b* $(NH_4)_3PMo_{12}$, *c* $BiPMo_{12}$, *d* $SbPMo_{12}$, *e* $SnPMo_{12}$

an effect on the ammonium salt formation. The P–O_a vibration of PO_4 tetrahedron is Raman-inactive. The observed vibration bands at 988 and 240 cm^{-1} are the most intense. In Raman spectroscopy, the dark colour of the $SbPMo_{12}$ and $SnPMo_{12}$ salts, reflecting their reduced state, does not permit their analysis as the incident beam is absorbed by the reduced sample [18].

UV–Visible diffuse reflectance seems to be a very appropriate technique to distinguish the electronic properties of the Mo ions. In the UV–Vis spectra of salts, prepared at pH 1 and pH 4 (Figs. 4, 5), a large band in the

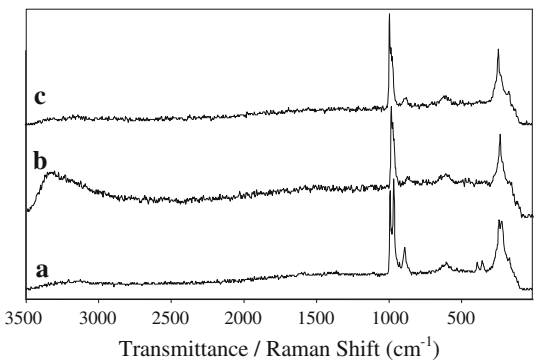

Fig. 3 Raman spectra of *a* $(NH_4)_3PMo_{12}$ prepared at pH 1, *b* $(NH_4)_3PMo_{12}$ prepared at pH 4, *c* $BiPMo_{12}$

domain of wavelengths 200–450 nm was observed with multiplicity for all samples. It is constituted of several components (200–250, 270–350 and 400–450 nm ranges) having different energies associated with ligand–metal charge transfers from oxygen to Mo(VI) in the Keggin anion. This result has been also observed by other authors that suggested that the presence of more than one band in the spectrum of Keggin-type compound is attributed to different oxygen ions (O_a, O_b, O_c and O_d) and to inter-anion charge transfer transitions [14, 18–21]. These energies have been also associated with cationic composition of the Keggin secondary framework, crystallinity of the compound and oxidation potential of the oxometal. In addition to this broad absorption band, another large charge transfer band was observed above 700 nm for both $SnPMo_{12}$ and $SbPMo_{12}$ samples that may be attributed to the d–d transition band of d^1 Mo(V) species in octahedral coordination [22–25]. This result suggested a partial reduction of Mo(VI) to Mo(V) in both $SnPMo_{12}$ and $SbPMo_{12}$ salts corresponding to the electron exchange occurring between Sb(III) or Sn(II) and Mo(VI) as follows:

$$Sn^{II} + 2Mo^{VI} \leftrightarrow Sn^{IV} + 2Mo^{V},\ Sb^{III} + 2Mo^{VI} \leftrightarrow Sb^{V} + 2Mo^{V}$$

In ^{31}P NMR analysis, $(NH_4)_3PMo_{12}$, prepared at pH 1(Fig. 6) and $BiPMo_{12}$ (Fig. 7), gave only one peak, at −4.4 ppm. The chemical shift of ^{31}P has been found at −4.4 ppm for $H_3PMo_{12}O_{40}$, a value close to those observed for our samples. However, for $(NH_4)_3PMo_{12}$, prepared at pH 4, $SnPMo_{12}$ and $SbPMo_{12}$ samples, their ^{31}P NMR spectrum could be decomposed in three peaks: one at −4.4 ppm, as major peak, and the two others, as minor peaks, at −1.6 and 7.8 ppm for $(NH_4)_3PMo_{12}$, at −5.89 and 0.6 ppm for $SbPMo_{12}$ and at −5.85 and 0.1 ppm for $SnPMo_{12}$. These results suggest either a slow decomposition of the Keggin anion at pH 4 or a presence of phosphor-based impurities. For $(NH_4)_3PMo_{12}$, prepared at pH 4, the peak at 7.8 ppm can be attributed to lacunary compound, $(NH_4)_7PMo_{11}O_{39}$. The results of chemical analysis of this salt (results no shown) showed an excess of ammonium ions. ^{31}P MAS NMR technique is very sensitive to local chemical environment and surrounding symmetry of phosphor compared with IR, Raman and UV–Visible spectroscopies.

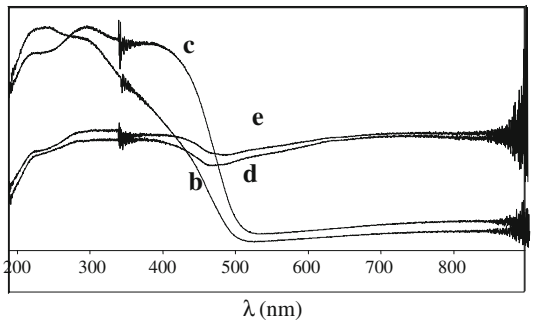

Fig. 5 UV–Visible spectra of $XPMo_{12}$ *b* $(NH_4)_3PMo_{12}$, *c* $BiPMo_{12}$, *d* $SbPMo_{12}$, *e* $SnPMo_{12}$

The thermal stability of salts was investigated by thermogravimetric (TG) and differential thermal analysis (DTA) (Fig. 8). The TG curves of two $(NH_4)_3PMo_{12}$ salts and that of $BiPMo_{12}$ (Fig. 8a–c) show that there are three steps of weight loss between 25 and 500 °C. Before 200 °C, the weight loss is attributed to crystallization water desorption and between 200 and 500 °C, the weight loss that was conducted in two steps, is assigned to ammonium ions' departure. In the DTA curves (Fig. 8a–c), in addition endothermic peaks associated with different mass losses observed in TG, exothermal signals assigned to the decomposition of salts to P_2O_5 and MoO_3 oxides, were observed with maximum at 488, 425 and 453 °C for $(NH_4)_3PMo_{12}$, prepared at pH 1, to that prepared at pH 4 and $BiPMo_{12}$, respectively. This study shows that $(NH_4)_3PMo_{12}$, prepared at pH 4, is the less stable. In the case of $SnPMo_{12}$ and $SbPMo_{12}$ salts (Fig. 8d, e), continuous weight loss is observed between 25 and 500 °C. The broad exothermic peaks with maxima at 449 and 503 °C are assigned to the complete decomposition of $SnPMo_{12}$ and $SbPMo_{12}$, respectively. The thermal stability of

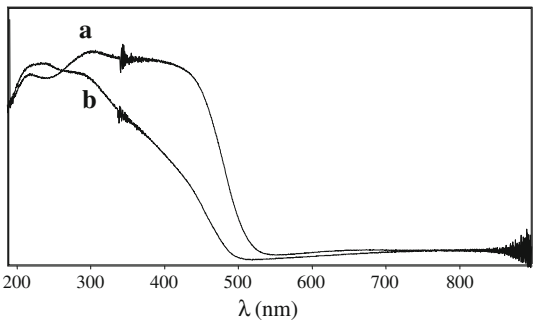

Fig. 4 UV–Visible spectra of $(NH_4)_3PMo_{12}O_{40}$; *a* prepared at pH 1, *b* prepared at pH 4

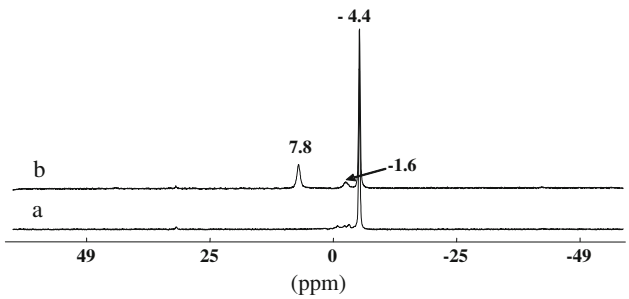

Fig. 6 ^{31}P MAS NMR spectra of $(NH_4)_3PMo_{12}O_{40}$ *a* prepared at pH 1, *b* prepared at pH 4

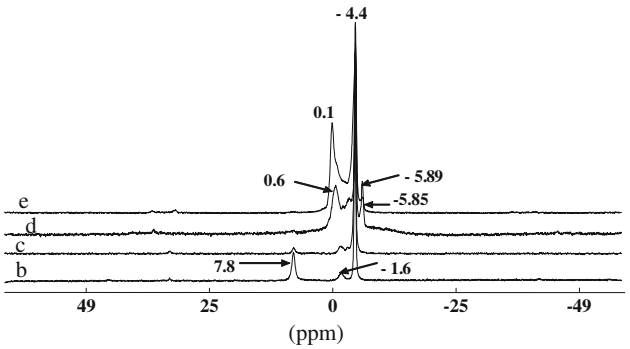

Fig. 7 ^{31}P MAS NMR spectra of $XPMo_{12}$ *b* $(NH_4)_3PMo_{12}$, *c* $BiPMo_{12}$, *d* $SbPMo_{12}$, *e* $SnPMo_{12}$

$SnPMo_{12}$ sample is the highest, probably due to strong reducing character of tin ions, as shown in UV–Visible.

The XRD patterns corresponding at 25, 200 and 400 °C (Fig. 9a) are characteristic of the ammonium salt prepared at pH 1 that crystallizes in a cubic system (JCPDS 09-0412). The XRD patterns of the ammonium salt prepared at pH 4, recorded at 25 °C and after thermal treatment at 200 °C (Fig. 9b), are similar to that of the ammonium salt prepared at pH 1, but with additional lines, in particular in the (2θ: 5–30°) domain. These lines disappear after a pretreatment at 400 °C and the cubic structure take place. The patterns of $XPMo_{12}$ salts (Fig. 10a–c) are similar to that of no substituted salt, prepared at pH 1, suggesting that $XPMo_{12}$ crystallizes in the same system (cubic). This observation confirms that X stabilizes the cubic structure. The XRD patterns of all salts, after treatment at 400 °C, show that the cubic structure was maintained. This indicates that all samples maintain their structure when most of ammonium cations were eliminated as observed in TG analysis. This phenomenon agrees with that observed by Sultan et al. [26]. After treatment at 450 °C, the XRD analysis shows the formation of molybdenum trioxide in the monoclinic form (β MoO_3) and in the

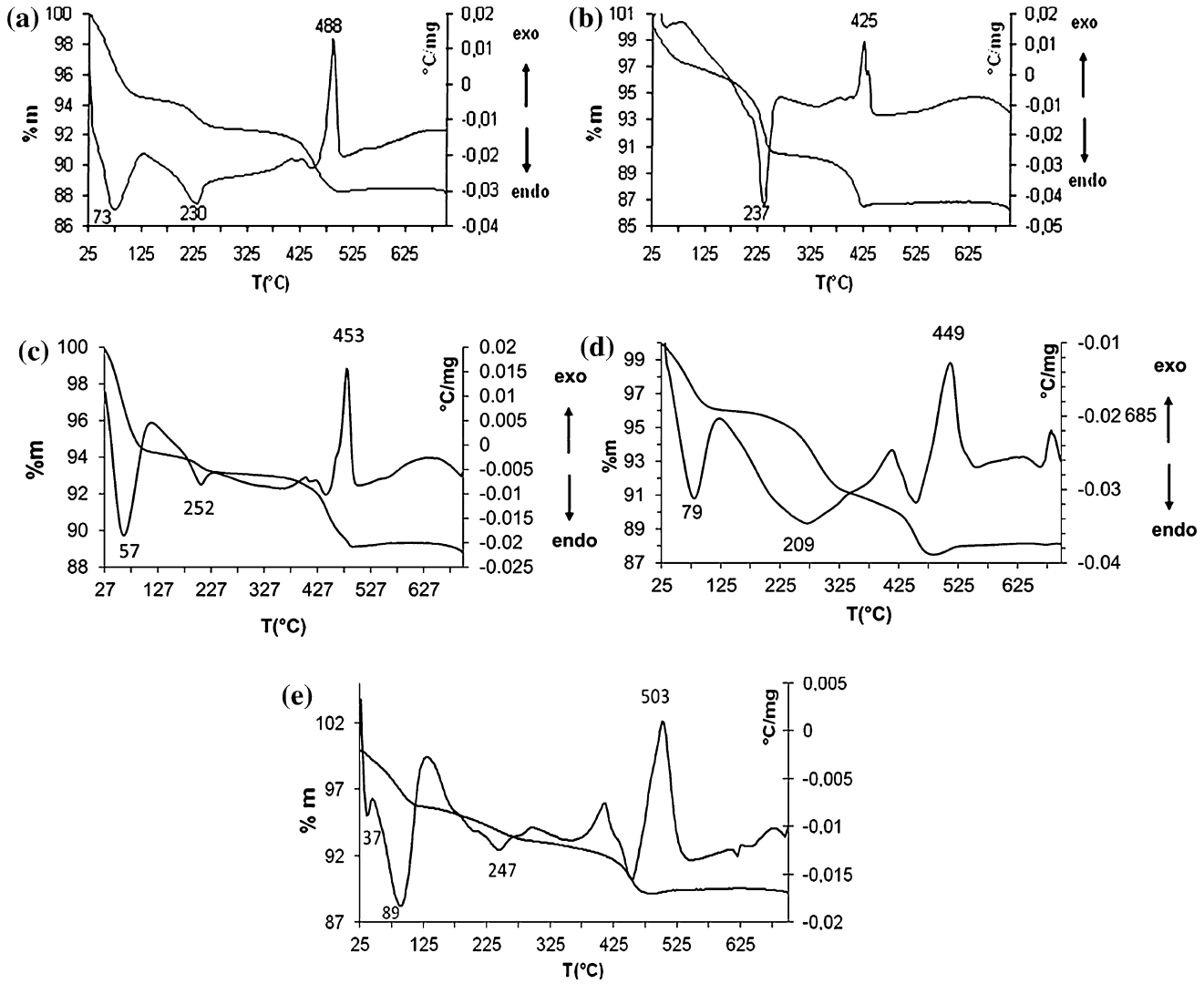

Fig. 8 TG–DTA diagrams of **a** $(NH_4)_3PMo_{12}$ prepared at pH 1, **b** $(NH_4)_3PMo_{12}$ prepared at pH 4, **c** $BiPMo_{12}$, **d** $SbPMo_{12}$, **e** $SnPMo_{12}$

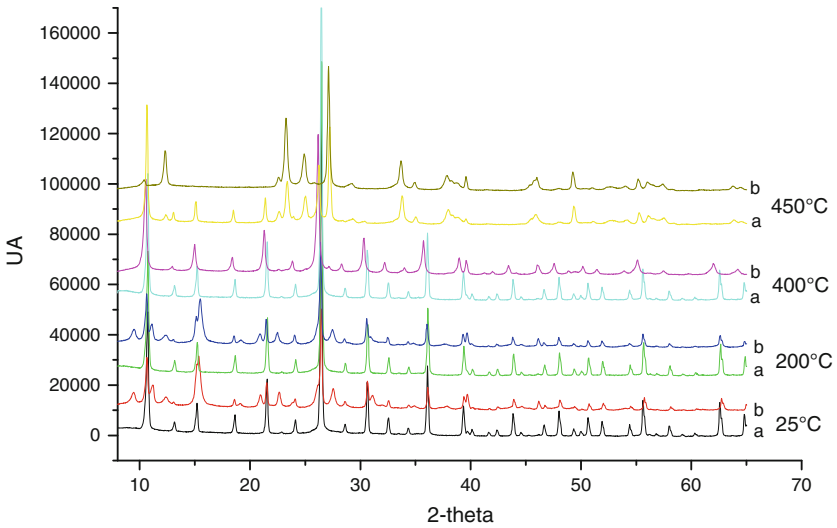

Fig. 9 XR patterns of $(NH_4)_3PMo_{12}O_{40}$ *a* prepared at pH 1, *b* prepared at pH 4

orthorhombic form (α MoO_3) whatever the salt composition. These two species (α and β MoO_3) were already observed by Rocchiccioli-Deltcheff et al. [27], in the case of the decomposition of 12-molybdophosphoric acid. After treatment at 500 °C, only orthorhombic α MoO_3 was detected, showing that β MoO_3 was transformed into α MoO_3.

The physicochemical characterizations of $(NH_4)_3PMo_{12}$, prepared at pH 4, are different of those of the other salts, suggesting probably that a lacunary compound was developed with the composition $(NH_4)_7PMo_{11}O_{39}$, in addition to that corresponding to salt, prepared at pH 1 ($(NH_4)_3PMo_{12}$) [15]. These results also showed that the partial substitution of the ammonium ions by Sn, Bi or Sb ions stabilizes the Keggin anion at pH 4, probably due to the X^{n+} ion hydrolysis that led to a decrease of the pH during the salt preparation.

Catalytic test

Decomposition of isopropanol occurs by two parallel reactions, the dehydration carried out in acidic sites giving the olefin (propene) and diisopropyl ether (DIPE) and the dehydrogenation to acetone occurring either in basic sites/concerted acid–base pair or redox sites [28–33]. On the other hand, it has been observed that strong Brönsted acid sites seem to catalyse the isopropanol decomposition to propene and weak acid sites to isopropyl ether via bimolecular recombination of isopropoxide species.

In this study, propene, diisopropyl ether and acetone are the observed reaction products with some selected catalysts. The obtained catalytic results (propan-2-ol conversion and product selectivities) on pretreated heteropoly salts under nitrogen in situ for 2 h at different temperatures (150–250 °C) and tested at 100 °C are shown in Figs. 11, 12 and Table 1.

Figure 11 shows that for all catalysts, the isopropanol conversion increases rapidly with pretreatment temperature and seems be nearly independent of reaction time, whatever the pretreatment temperature. Moreover, the isopropanol decomposition proceeded without catalyst deactivation. These results emphasize the increase of the density or the acidity strength of active sites with pretreatment temperature and emphasize also the high stability of HPSs.

Figure 12 shows also that for all catalysts, bimolecular reaction to form isopropyl ether also seems be nearly independent of reaction time whatever the pretreatment temperature. The same observation was made on the isopropanol dehydration to propene (Figure not shown). These results suggest that the DIPE formation requires acid sites different from those of the alcohol dehydration to propene. Therefore, both reactions occur in parallel: one requiring weak acid sites (in the case of DIPE) and the other strong acid sites (in the case of propene), based on the results reported by some authors [32, 33].

All data of Table 1 were collected after 5 h of reaction. For the catalysts prepared at pH 4, the conversion passes from ca. 2–7 % to ca. 70–94 % when the pretreatment temperature increases from 150 to 250 °C, showing a high concentration of active sites at high pretreatment temperature. It is noteworthy that $(NH_4)_3PMo_{12}$, prepared at pH 1, is active at low pretreatment temperature (150 °C) with ca. 49 % against ca. 2 % of conversion for those prepared at pH 4. These results cannot be explained on the basis of the structure of salts (cubic system) because it does not change in the 25–400 °C temperature range, as shown by XRD analysis and on the basis BET surface areas values, since no parallel is observed with the conversion values. However, this can be explained by the concept 'pseudoliquid' catalysis [13]. The pretreatment of the catalyst at 250 °C

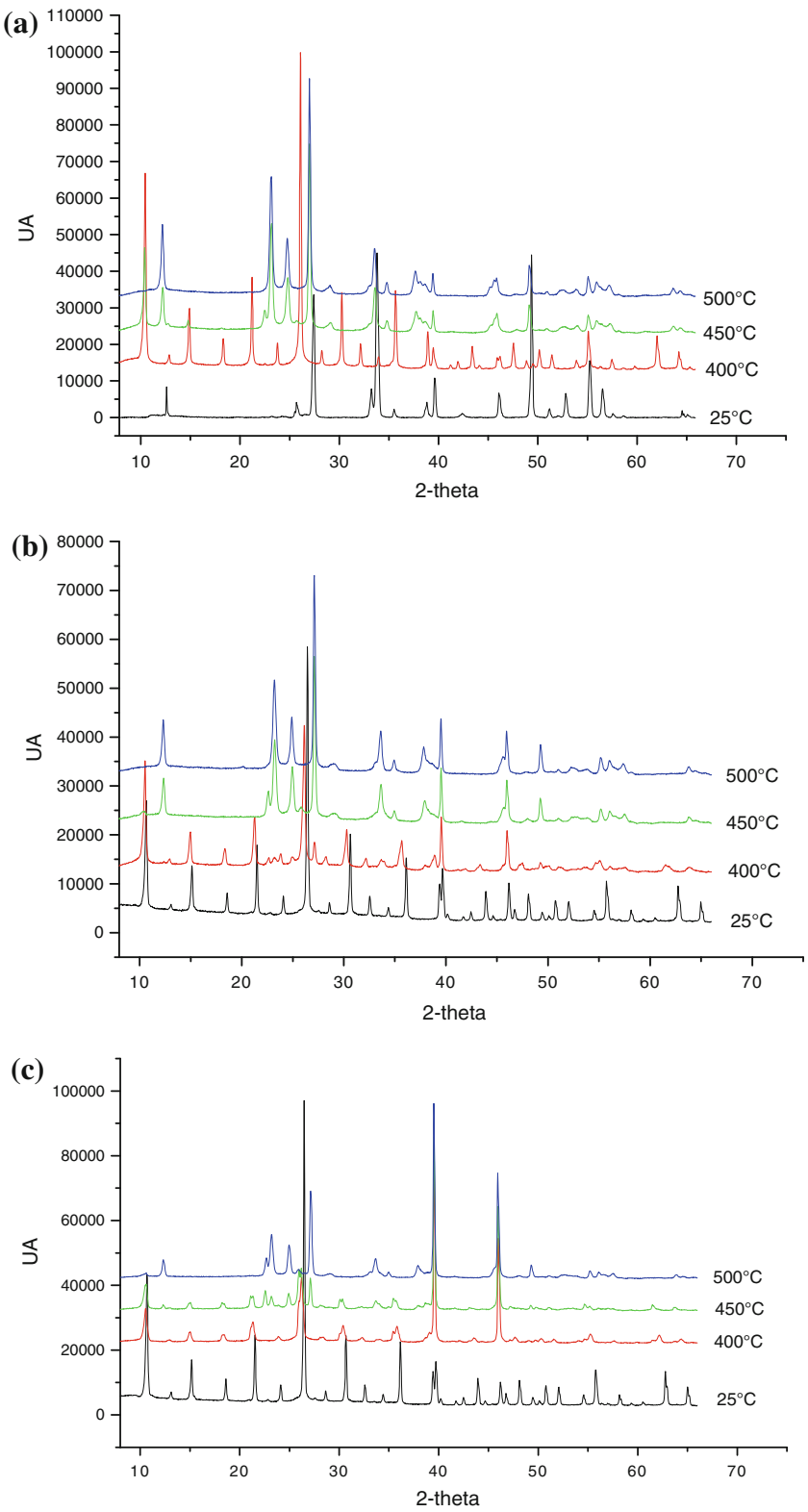

Fig. 10 XR patterns of **a** $BiPMo_{12}$, **b** $_{12}$ **c** SnPMo

has probably caused an increase in the volume of the crystal lattice and, therefore, a strong absorption and a high isopropanol concentration into the solid bulk to undergo the decomposition. On the other hand, it was reported that the polar molecules like alcohols are readily absorbed into the solid bulk expanding the distance between the polyanions after the total departure of water molecules.

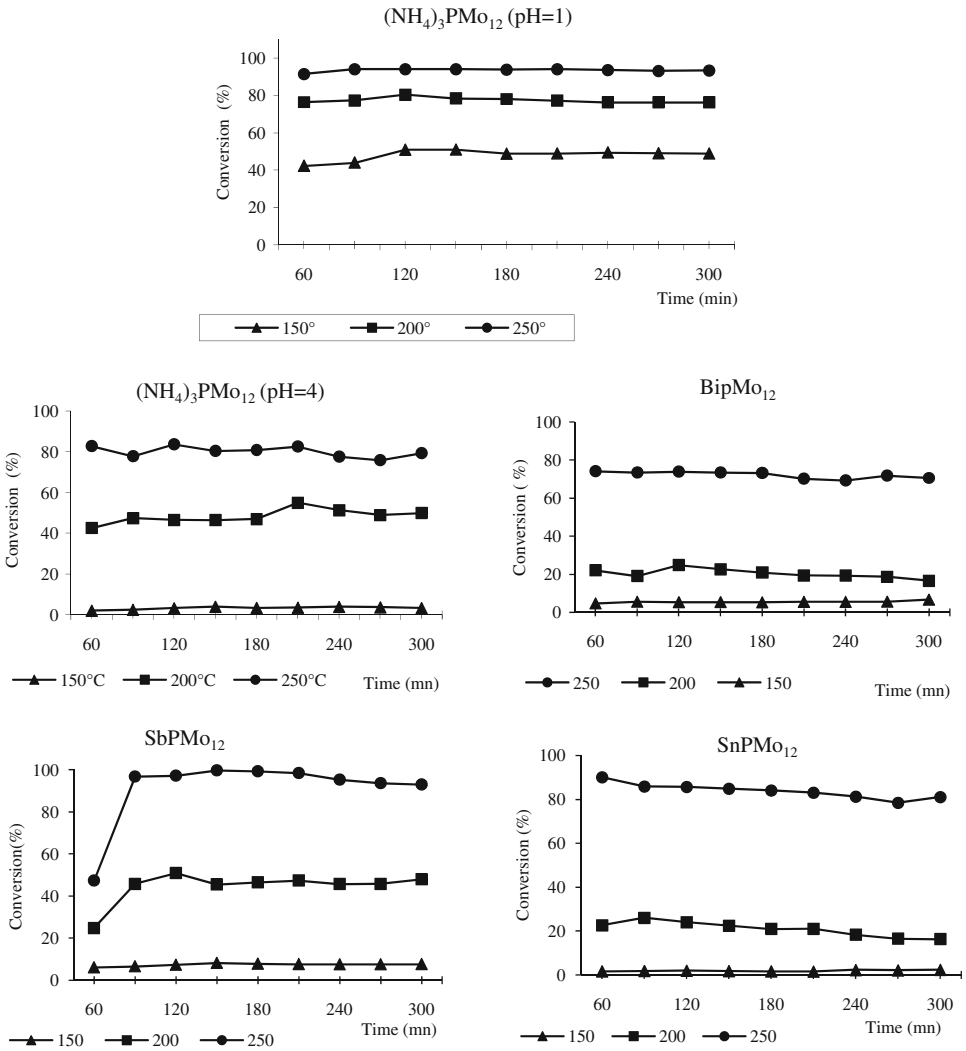

Fig. 11 Conversion of isopropanol as function of time at 100 °C for various catalysts

The product distribution is very sensitive to both pre-treatment temperature and chemical composition of salt (Table 1). As for the catalytic activity, propene selectivity increases from ca. 23–44 to ca. 51–95 % with the pre-treatment temperature (from 150 to 250 °C), for all catalysts. These results indicate that a high pretreatment temperature leads to strong acid sites favoring the formation of propene.

The acetone, dehydrogenation product, is mainly observed for salts prepared at pH 4, when the pre-treatment temperature is low (150 °C) with selectivities of ca. 32–65 %. The obtained high selectivity in the presence of $SnPMo_{12}$ (65 %) can be attributed to the high reducing power of the ion Sn(II) and consequently to the simultaneous presence of redox couples, Mo(VI)/Mo(V) and Sn(IV)/Sn(II) as observed by UV–Visible spectroscopy. These active sites favouring the dehydrogenation activity decrease strongly to the detriment of those that promote isopropanol dehydration, when the pretreatment temperature increases.

While, the appearance of acid sites favourable to DIPE formation seems to depend on the operating conditions and the composition of the catalyst. In the case of $(NH_4)_3PMo_{12}$, DIPE selectivity decreases from ca. 74 to ca. 5 % with increase of pretreatment temperature from 150 to 250 °C with the salt prepared at pH 1, unlike to that prepared at pH 4, where the highest selectivity to DIPE was observed at a pretreatment temperature of 200 °C (ca. 64 % against ca. 34 and ca. 41 % for 150 and 250 °C respectively). In the case of substituted salts, for a temperature of 150 °C, isopropanol dehydration toward DIPE is not observed in the presence of $SnPMo_{12}$, while it is of ca. 22 and ca. 43 % in the presence of $SbPMo_{12}$ and $BiPMo_{12}$, respectively. For all salts, a pretreatment temperature of 200 °C generates more acid sites favourable to the DIPE formation with a selectivity of ca. 35, 47 and 72 % for $SnPMo_{12}$, $BiPMo_{12}$ and $SbPMo_{12}$, respectively. For a pretreatment temperature of 250 °C, $BiPMo_{12}$ is the most selective with ca. 45 against ca. 28 and 7 % for $SnPMo_{12}$ and $SbPMo_{12}$, respectively.

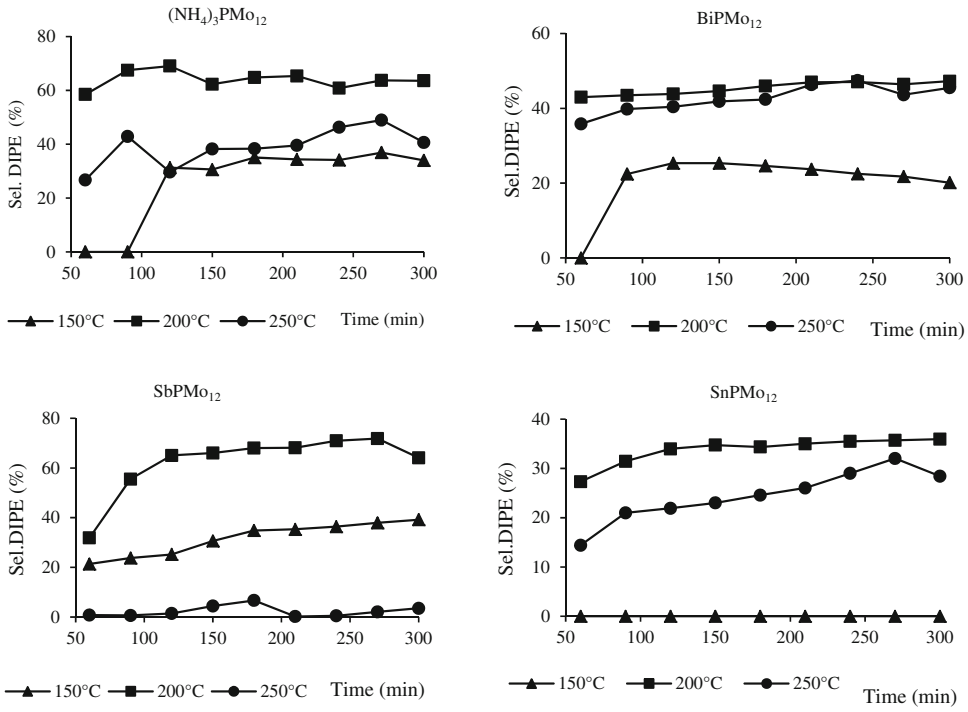

Fig. 12 Selectivity of DIPE as function of time at 100 °C for various catalysts

Table 1 Propan-2-ol conversion and product selectivities as a function of pretreatment temperature on Keggin POMs

Catalysts	Pre-treatment temperature (°C)	Conversion (%)	Selectivities (yield[a]) (%)		
			Propene (%)	DIPE (%)	Acetone (%)
$(NH_4)_3PMo_{12}$ (pH 1)	150	48.8	23.0 (11.2)	73.7 (36.0)	3.3 (1.6)
	200	76.3	36.9 (28.2)	60.5 (46.2)	2.6 (2.0)
	250	93.4	94.9 (88.6)	5.1 (4.8)	0.0 (0.0)
$(NH_4)_3PMo_{12}$ (pH 4)	150	3.2	31.5 (1.0)	34.0 (1.1)	34.5 (1.1)
	200	50.0	34.8 (17.4)	63.6 (31.8)	1.6 (0.8)
	250	79.0	58.1 (45.9)	41.0 (32.4)	0.9 (0.7)
$BiPMo_{12}$	150	5.5	44.0 (2.4)	22.0 (1.2)	34.0 (1.9)
	200	19.5	49.0 (9.6)	47.0 (9.2)	4.0 (0.8)
	250	70.5	51.2 (36.1)	45.5 (32.1)	3.3 (2.3)
$SbPMo_{12}$	150	7.3	24.0 (1.8)	43.5 (3.2)	32.5 (2.4)
	200	45.8	25.0 (11.5)	71.9 (32.9)	3.2 (1.5)
	250	94.5	90.9 (85.9)	6.7 (6.3)	2.4 (2.3)
$SnPMo_{12}$	150	2.2	35.0 (0.8)	0.0 (0.0)	65.0 (1.4)
	200	18.3	50.6 (9.3)	35.5 (6.5)	13.9 (2.5)
	250	81.0	67.2 (54.4)	28.4 (23.0)	4.3 (3.5)

Reaction conditions: reaction temperature: 100 °C, pretreatment: 2 h/N_2 (2 l/h), catalyst weight: 200 mg, total flow rate: 1 l/h.

[a] Yield $= \frac{\text{conversion} \times \text{selectivities}}{100}$

The comparison of catalytic behaviour of $XPMo_{12}$ salts shows that the highest DIPE yields are obtained for $SbPMo_{12}$, pretreated at 200 °C (ca. 33 %) and for $BiPMo_{12}$ and $SnPMo_{12}$ pretreated at 250 °C (ca. 32 and 23 % respectively). The presence of active acid sites favourable to DIPE formation can be attributed to water coordination of both X^{n+} and NH_4^+ ions. Pretreated at 200 or 250 °C, the catalyst still retains the water of coordination of X^{n+} ions in addition the ammonium ions as observed by thermal analysis. Niiyama et al. [34] showed that the dehydrating activity of a solid may be related to water coordination of M^{n+} ions that generates protons from the following equation:

$$\left[M(H_2O)_m\right]^{n+} \rightarrow \left[M(H_2O)_{m-1}(OH)\right]^{(n-1)+} + H^+$$

It is known that the hydrated ions are weak Brönsted acids. When the coordination water of X^{n+} ions is removed, the weak Brönsted acid sites are transformed into Lewis acid sites that favour the formation of propene.

The catalytic results showed that the pretreatment temperature is an important factor to take into consideration with this type of material and also showed their ability to absorb and desorb rapidly the reagent and the reaction products, respectively, at low reaction temperature (100 °C) without changes in overall bulk crystal structure. On the other hand, the pH increase in the $(NH_4)_3PMo_{12}$ salt preparation seems not to have a strong effect on their catalytic properties.

Conclusion

The physicochemical characterizations of substituted salts, $XPMo_{12}$, prepared at pH 4 are similar to those of $(NH_4)_3PMo_{12}$, prepared at pH 1, showing that the pH has no effect on the structure of Keggin anion and on that of polyoxometalate. With a pH 4, the $(NH_4)_7PMo_{11}O_{39}$ lacunary compound seems to be obtained.

It was shown in this work that based ammonium salts of 12-molybdophosphoric acid are effective for the direct isopropanol decomposition to DIPE compared to traditional etherification catalysts such as highly acidic ion exchange resins and strong mineral acids that are polluting and corrosive.

References

1. Johnson R, Pankow J, Bender D, Price C, Zogorski J (2000) MTBE: to what extent will past releases contaminate community supply wells? Environ Sci Technol 34:210A
2. Child JE, Choi BC, Ragonese FP (1990) Dual stage process for the production of ethers. US Patent 4935552
3. Taylor RJ, Jr, Dai PE, Knifton JF (1996) Integrated process for the production of isopropyl alcohol and diisopropyl ethers. US Patent 5583266
4. Taylor RJ, Dai PE, Knifton JF (2000) Diisopropyl ether one-step generation from acetone-rich feedstocks. Catal Lett 68:1–5
5. Chidambaram V, Viswanathan B (2007) Single step catalytic production of diisopropyl ether (DIPE) from acetone feedstock over nickel based catalysts. Appl Catal B: Environ 71:32–43
6. Heese FP, Dry ME, Möller KL (1999) Single stage synthesis of diisopropyl ether: an alternative octane enhancer for lead-free petrol. Catal Today 49:327–335
7. Heese FP, Dry ME, Möller KL (2000) The mechanism of diisopropyl ether synthesis from a feed of propylene and isopropanol over ion exchange resin. Stud Surf Sci Catal 130C:2597–2602
8. Jarecka T, Miescheriakow ST, Datka J (2000) Acid and catalytic properties of supported sulfopolyphenylketones in the formation of DIPE, MTBE and TAME ethers. Stud Surf Sci Catal 130C:2615–2620
9. Ortiz-Islas E, Lopez T, Navarrete J, Bokhimi X, Gomez R (2005) High selectivity to isopropyl ether over sulfated Titania in the isopropanol decomposition. J Mol Catal A/Chem 228:345–350
10. Bielanski A, Lubanska A, Pozniczek J, Micek-Ilnicka A (2003) Oxide supports for 12-tungstosilicic acid catalysts in gas phase synthesis of MTBE. Appl Catal A: Gen 238:239–250
11. Bielanski A, Lubanska A, Micek-Ilnicka A, Pozniczek J (2005) Polyoxometalates as the catalysts for tertiary ethers MTBE and ETBE synthesis. Coord Chem Rev 249:2222–2231
12. Lopez-Salinas E, Hernandez-Cortez JG, Navarrete J, Salmon M, Schifter I (2000) Formation of diisopropyl ether from 2-propanol using Keggin-type $H_3[W_{12}PO_{40}]$ and $H_4[W_{12}SiO_{40}]$ heteropolyacids supported on Zirconia. Stud Surf Sci Catal 130C:2591–2596
13. Misono M (1987) Heterogeneous catalysis by heteropoly compounds of molybdenum and tungsten. Catal Rev Sci Eng 29:269
14. Dermeche L, Thouvenot R, Hocine S, Rabia C (2009) Preparation and characterization of mixed ammonium salts of Keggin phosphomolybdate. Inorg Chim Acta 362:3896–3900
15. Cavani F, Etienne E, Mezzogori R, Pigamo A, Trifiro F (2001) Improvement of catalytic performance in isobutane oxidation to methacrylic acid of Keggin-type phosphomolybdates by preparation via lacunary precursors: nature of the active sites. Catal Lett 75:1–2
16. Rocchiccioli-Deltcheff C, Fournier M, Frank R, Thouvenot R (1983) Vibrational investigations of polyoxometalates. 2. Evidence for anion-anion interactions in molybdenum (VI) and tungsten (VI) compounds related to the Keggin structure. Inorg Chem 22:207–216
17. Rocchiccioli-Deltcheff C, Thouvenot R, Frank R (1976) Spectres IR et Raman d'hétéropolyanions α-$XM_{12}O_{40}^{n-}$ de structure de type Keggin (X = B^{III}, Si^{IV}, Ge^{IV}, P^{V}, As^{V} et M = W^{VI} et Mo^{VI}). Spectrochim Acta 32A:587–597
18. Rocchiccioli-Deltcheff C, Aouissi A, Bettahar MM, Launay S, Fournier M (1996) Catalysis by 12-molybdophosphates: 1. catalytic reactivity of 12-molybdophosphoric acid related to its thermal behavior investigated through IR, Raman, polarographic, and X-ray diffraction studies: a comparison with 12-molybdosilicic acid. J Catal 164:16–27
19. Cavani F, Mezzogori R, Pigamo A, Trifiro F (2001) Improved catalytic performance of Keggin-type polyoxometalates in the oxidation of isobutane to methacrylic acid under hydrocarbon-lean conditions using antimony-doped catalysts. Chem Eng J 82:33–42
20. Srilakshmi CH, Lingaiah N, Suryanarayana I, Sai Prasad PS, Ramesh K, Anderson BG, Niemantsverdriet JW (2005) In situ synthesis of ammonium salt of 12-molybdophosphoric acid on iron phosphate and the ammoxidation functionality of the catalyst in the transformation of 2-methylpyrazine to 2-cyanopyrazine. Appl Catal A: Gen 296:54–62
21. Fournier M, Louis C, Che M, Chaquin P, Masure D (1989) Polyoxometalates as models for oxide catalysts: Part I. An UV-visible reflectance study of polyoxomolybdates: influence of polyhedra arrangement on the electronic. J Catal 119:400
22. Mazari T, Marchal-Roch C, Hocine S, Salhi N, Rabia C (2009) Oxidation of propane over substituted Keggin phosphomolybdate salts. J Nat Gas Chem 18:319–324
23. Carmen Cabelloa I, Irma Botto L, Horacio Thomas J (2000) Anderson type heteropolyoxomolybdates in catalysis: 1. $(NH_4)_3[CoMo_6O_{24}H_6]\cdot 7H_2O/\gamma$-$Al_2O_3$ as alternative of Co-Mo/γ-Al_2O_3 hydrotreating catalysts. App Catal A 197:79–86
24. Thomazeau C, Martin V, Afanasiev P (2000) Effect of support on the thermal decomposition of $(NH_4)_6Mo_7O_{24}\cdot 4H_2O$ in the inert gas atmosphere. Appl Catal A: Gen 199:61–72
25. Cavani F, Mezzogori R, Pigamo A, Trifiro F, Etienne E (2001) Main aspects of the selective oxidation of isobutane to

methacrylic acid catalyzed by Keggin-type polyoxometalates. Catal Today 71:97–110
26. Sultan M, Paul S, Fournier M, Vanhove D (2004) Evaluation and design of heteropoly compound catalysts for the selective oxidation of isobutane into methacrylic acid. Appl Catal A: Gen 259:141–152
27. Rocchiccioli-Deltcheff C, Aouissi A, Launay S, Fournier M (1996) Silica-supported 12-molybdophosphoric acid catalysts: influence of the thermal treatments and of the Mo contents on their behavior, from IR, Raman, X-ray diffraction studies, and catalytic reactivity in the methanol oxidation. J Mol Catal A Chem 114:331–342
28. Wang JA, Bokhimi X, Novaro O, López T, Gómez R (1999) Effects of the surface structure and experimental parameters on the isopropanol decomposition catalyzed with sol–gel MgO. J Mol Catal 145:291–300
29. Shyamal KB, Christopher AB, Levi TT (2003) Acid and base characteristics of molybdenum carbide catalysts. Appl Catal A 250:197–208
30. Liu SY, Yang SM (2008) Complete oxidation of 2-propanol over gold-based catalysts supported on metal oxides. Appl Catal A: Gen 334:92–99
31. Dominguez MI, Sanchez M, Centeno MA, Montes M, Odriozola JA (2007) 2-Propanol oxidation over gold supported catalysts coated ceramic foams prepared from stainless steel wastes. J Mol Catal A chem 277:145–154
32. Sun Q, Fu Y, Liu J, Auroux A, Shen J (2008) Structural, acidic and redox properties of V_2O_5–TiO_2–SO_4^{2-} catalysts. Appl Catal A: Gen 334:26–34
33. Rioux RM, Vannice MA (2005) Dehydrogenation of isopropyl alcohol on carbon-supported Pt and Cu–Pt catalysts. J Catal 233:147–165
34. Niiyama H, Saito Y, Echigoya E (1981) Proceedings, 7th International Congress on Catalysis, Tokyo, 1980. Elsevier, Amsterdam, p 1416